Neurobiology of Stress 15 (2021) 100415

Contents lists available at ScienceDirect

Neurobiology of Stress

journal homepage: www.elsevier.com/locate/ynstr

Neurochemically distinct populations of the bed nucleus of stria terminalis modulate innate fear response to weak threat evoked by predator odor stimuli

Biborka Bruzsik [a,b], Laszlo Biro [a,c], Klara Rebeka Sarosdi [a], Dora Zelena [d,e], Eszter Sipos [d], Huba Szebik [a,b], Bibiána Török [b,d], Eva Mikics [a,1], Mate Toth [a,*,1]

[a] Laboratory of Translational Behavioural Neuroscience, Institute of Experimental Medicine, Budapest, Hungary
[b] Janos Szentagothai Doctoral School of Neurosciences, Semmelweis University, Budapest, Hungary
[c] Laboratory of Thalamus Research, Institute of Experimental Medicine, Budapest, Hungary
[d] Laboratory of Behavioural and Stress Studies, Institute of Experimental Medicine, Budapest, Hungary
[e] Center for Neuroscience, Szentágothai Research Center, Institute of Physiology, Medical School, University of Pécs, Pécs, Hungary

ARTICLE INFO

Keywords:
Bed nucleus of stria terminalis
Innate fear
Threat detection
Anxiety
Defensive response
Predator scent

ABSTRACT

Anxiety and trauma-related disorders are characterized by significant alterations in threat detection, resulting in inadequate fear responses evoked by weak threats or safety stimuli. Recent research pointed out the important role of the bed nucleus of stria terminalis (BNST) in threat anticipation and fear modulation under ambiguous threats, hence, exaggerated fear may be traced back to altered BNST function. To test this hypothesis, we chemogenetically inhibited specific BNST neuronal populations (corticotropin-releasing hormone - $BNST^{CRH}$ and somatostatin - $BNST^{SST}$ expressing neurons) in a predator odor-evoked innate fear paradigm. The rationale for this paradigm was threefold: (1) predatory cues are particularly strong danger signals for all vertebrate species evoking defensive responses on the flight-avoidance-freezing dimension (conservative mechanisms), (2) predator odor can be presented in a scalable manner (from weak to strong), and (3) higher-order processing of olfactory information including predatory odor stimuli is integrated by the BNST. Accordingly, we exposed adult male mice to low and high predatory threats presented by means of cat urine, or low- and high-dose of 2-methyl-2-thiazoline (2MT), a synthetic derivate of a fox anogenital product, which evoked low and high fear response, respectively. Then, we tested the impact of chemogenetic inhibition of $BNST^{CRH}$ and $BNST^{SST}$ neurons on innate fear responses using crh- and sst-ires-cre mouse lines. We observed that $BNST^{SST}$ inhibition was effective only under low threat conditions, resulting in reduced avoidance and increased exploration of the odor source. In contrast, $BNST^{CRH}$ inhibition had no impact on 2MT-evoked responses, but enhanced fear responses to cat odor, representing an even weaker threat stimulus. These findings support the notion that BNST is recruited by uncertain or remote, potential threats, and CRH and SST neurons orchestrate innate fear responses in complementary ways.

1. Introduction

Psychiatric conditions related to exaggerated or context-inadequate fear responses exhibit significant alterations of threat detection, i.e. how actual or potential threats are perceived and interpreted (Levy and Schiller, 2021). Since detection of life-threatening signals has been essential for survival throughout phylogenetic evolution, highly conserved regulatory mechanisms have been formed in the brain (Pereira and Moita, 2016). Predatory cues are universal danger signals in all vertebrate species including humans, modulating behavioral responses on the approach-avoidance dimension (e.g. exploration vs hiding) with significant autonomic and hypothalamic-pituitary-adrenal (HPA) axis activation (Apfelbach et al., 2005, 2015; Bach et al., 2014; Pereira and Moita, 2016). Neurobiological mechanisms regulating defensive responses have been well-characterized across species, offering potentials for translational research by deeper understanding how

* Corresponding author. Laboratory of Translational Behavioural Neuroscience, Institute of Experimental Medicine, Budapest-1083, Hungary.
E-mail address: toth.mate@koki.hu (M. Toth).
[1] Eva Mikics and Mate Toth contributed equally to this work.

https://doi.org/10.1016/j.ynstr.2021.100415
Received 19 July 2021; Received in revised form 26 October 2021; Accepted 27 October 2021
Available online 29 October 2021
2352-2895/© 2021 The Author(s). Published by Elsevier Inc. This is an open access article under the CC BY-NC-ND license (http://creativecommons.org/licenses/by-nc-nd/4.0/).

adaptive vs maladaptive innate defensive responses are formed. Predator-related sensory signals (e.g. looming as visual, alarm calls as auditory, or urinary scent as olfactory stimuli) reach the amygdala through colliculo-thalamic or direct olfactory pathways, which conveys sensory information with additional valence to hypothalamic centres (ventromedial and premammilary regions), where defensive behavioral responses are initiated and executed via the brainstem, i.e. peri-aqueductal grey, autonomic centres, and motor nuclei (Pereira and Moita, 2016; Silva et al., 2016). Despite detailed neuroanatomical schematics of innate defensive responses, modulation of responses according to actual threats (i.e. along the 'flight--approach-avoidance-immobility' dimension) is less understood. Latter is mainly determined by the proximity of the predator in a natural setting (Fanselow and Lester, 1988). Recent findings also suggest that a major difference between adaptive vs maladaptive fear response is the low vs high threshold for threatening signals (e.g. earlier escape) (Fung et al., 2019; Mobbs et al., 2010).

Recent research pointed out the important role of the bed nucleus of stria terminalis (BNST) in the regulation of emotional states and behavioral responses under threatening conditions, particularly when the threat is more ambiguous or remote, and behavior is formed in the anticipation of *potential* danger (Goode et al., 2019, 2020; Klumpers et al., 2017; Mobbs et al., 2010). Neuroanatomical localization and connections of the BNST, i.e. as an interface between integrative and executive centers (Cullinan et al., 1993; Janitzky et al., 2015; Miller et al., 2019; Radley et al., 2009), also imply its modulatory role in threat detection and adequate action selection, i.e. how sensory information with negative valence is translated into adaptive behavioral response (Alheid and Heimer, 1988; Daniel and Rainnie, 2016). Moreover, BNST is a higher-order sensory center of olfactory signals, including predatory odors (kairomones), exhibiting marked activity under predatory threat conditions (Asok et al., 2013; Day et al., 2004; Fendt et al., 2002; Giardino et al., 2018; Janitzky et al., 2015; Kobayakawa et al., 2007; Rale et al., 2017). Since the chemical nature and concentration of predator odor inform prey animals about the spatio-temporal proximity of predatory threat (Apfelbach et al., 2015; Fanselow and Lester, 1988), predator odor can be used as a scalable threat signal inducing innate fear responses in laboratory settings (Takahashi et al., 2005; Wallace and Rosen, 2000). As shown before, low risk signals tend to promote active risk assessment and 'cautious' behavior, whereas high-risk signals facilitate freezing or flight (Apfelbach et al., 2005; Lima and Bednekoff, 1999). Noteworthy, predator odor stimuli are significant stressors shaping behavioral reactivity on the long-term as shown by animal models of post-traumatic stress disorder (PTSD) (Cohen et al., 2014; Deslauriers et al., 2018; Janitzky et al., 2015).

Based on the above, we aimed to explore how the BNST modulates innate fear responses for predator odor, considered as an ecologically valid laboratory paradigm. In order to dissect the differential role of BNST under low and high threat conditions, we used a single molecule, 2-methyl-2-thiazoline (2MT), as a scalable threat stimulus. 2MT is a synthetic derivate of 2,5-dihydro-2,4,5-trimethylthiazoline (TMT), a widely-used fox anogenital compound evoking innate fear response (Apfelbach et al., 2015; Rosen et al., 2015). We used 2MT because of its potential to reliably induce freezing behavior (with elevated corticosterone levels) besides avoidance (particularly in mice) as shown by previous studies (Cruz et al., 2020; Isosaka et al., 2015; Zhong et al., 2018). Latter enabled us to monitor a more diverse behavioral repertoire by defining multiple variables on the approach-avoidance-freezing dimension. Since the BNST is a neurochemically heterogeneous structure expressing several neuropeptides (Gungor and Pare, 2016; Nguyen et al., 2016; Ye and Veinante, 2019), we focused our manipulations on distinct cell populations. We targeted somatostatin (SST) and corticotropin-releasing hormone (CRH) positive neurons based on previous reports showing their opposing role in active-passive fear response selection. SST neurons in the amygdala and prefrontal cortex have been shown to enhance passive fear and coping responses such as freezing and immobile states, or repress active avoidance (Ahrens et al., 2018; Cummings and Clem, 2020; Fadok et al., 2017; Hartley et al., 2019; Yu et al., 2016). Recently, we also found that SST neurons in the BNST enhance passive fear response (i.e. freezing) formation in a conditioned fear paradigm (Bruzsik et al., 2021). In contrast, CRH neurons seem to exert a complementary function, predominantly facilitating fear extinction, escape/flight behavior, and active defense (Daviu et al., 2020; Fadok et al., 2017; Hartley et al., 2019). However, the role of these cell populations in the BNST in shaping behavioral responses to threatening stimuli is still unclear. To test the stimulus-dependent modulatory role of these two neuronal populations, we chemogenetically inhibited SST and CRH neurons of the BNST under low and high threat conditions.

2. Materials and methods

2.1. Subjects

Adult (>8 weeks old) male C57Bl/6J mice, as well as crh-ires-cre and sst-ires-cre male mice on C57Bl/6J background (Jackson Laboratory, USA) were used in the present study (Taniguchi et al., 2011; Vong et al., 2011). All animals were group-housed (3–4 mice/cage) in Plexiglass chambers at constant temperature (22 ± 1 °C) and humidity (40–60%) under a reverse circadian light-dark cycle (lights-off at 7:00 a.m., lights-on at 7:00 p.m.). Mice were isolated 3 days before the first behavioral test and were kept single-housed during the testing period to prevent social buffering/modulatory effects. All behavioral tests were performed during the first half of the active (dark) cycle. Regular laboratory chow (Sniff, Soest, Germany) and tap water were available *ad libitum*.

Experiments were carried out in accordance with the European Communities Council Directive recommendations for the care and use of laboratory animals (2010/63/EU) and were reviewed and approved by the Animal Welfare Committee of the Institute of Experimental Medicine.

2.2. Stereotaxic surgery

Mice underwent stereotaxic surgery to bilaterally inject virus constructs into the BNST (anteroposterior +0.8 mm, mediolateral ±0.8 mm, dorsoventral −4.2 mm to Bregma; (Paxinos and Franklin, 2001)). Animals were anesthetized with a ketamine-xylazine solution (16.6 mg/ml ketamine and 0.6 mg/ml xylazine-hydrochloride in 0.9% saline, 10 ml/kg body weight intraperitoneally-i.p.) and placed in a stereotaxic frame (David Kopf Instruments, Tujunga, CA, USA). Viral vectors (20–40 nl volume/hemisphere) were microinjected through a glass pipette (tip diameter: 20–30 μm) at a rate of 100 nl/min by using a Nanoject II precision microinjector pump (Drummond, Broomall, PA, USA). The pipette was left in place for an additional 3 min to ensure diffusion before slow retraction. After the surgeries, mice received buprenorphine injection (Bupaq; 0.1 mg/kg) subcutaneously as analgesic treatment. Behavioral experiments were conducted 4–6 weeks after virus injection to allow time for gene expression.

2.3. Virus vectors

Adeno-associated viruses (AAVs) carrying Cre-inducible (double-inverse orientation; DIO) transgenes were purchased from Addgene (Watertown, MA, USA). We used AAV8-hSyn::DIO-hM4Di-mCherry (1.9e13 GC/ml titer, #44362) and AAV8-hSyn::DIO-mCherry (4.1e12 GC/ml titer, #50459) constructs to express inhibitory 'Designer Receptors Exclusively Activated by Designer Drugs' (DREADD) receptors or inactive control fluorophore.

2.4. Drugs

Designer receptor-ligand clozapine-N-oxide (CNO, Tocris Bioscience; 4936, CAS No: 34233-69-7) was freshly dissolved in 0.9% saline solution at a concentration of 0.3 mg/ml and administered in 10 ml/kg volume intraperitoneally (i.e. effective dose of 3 mg/kg) 40 min before behavioral testing.

2.5. Behavioral testing

2.5.1. Open field test

We assessed exploratory activity and anxiety-like behavior without predator stimuli in an open field arena under medium-light intensity (120 lux). The arena was made of white plastic (40 × 30 × 15 cm), which was cleaned with water and wiped dry between tests. Mice were placed in the corner and were allowed to explore the arena for 10 min. The inner 20 × 15 cm zone was considered as center, and time spent here was an index of anxiety. We defined three further behavioral variables to consistently measure exploratory activity and fear response across tests (i.e. with predatory stimuli exposures): (1) locomotor/horizontal exploratory activity (total distance moved in cm), (2) vertical exploratory activity (time spent with rearing), (3) time spent with immobility/freezing. All behavioral variables were quantified using EthoVision XT 15 software except rearing, which was hand-scored by an experimenter blind to treatment groups (Solomon Coder, Hungary; https://solomoncoder.com/). Freezing was defined by lack of movement using previously defined software settings and thresholds, which were validated by correlating Ethovision output data with expert hand-scoring (Spearman R > 0.9).

2.5.2. Predator odor test using cat urine or 2-methyl-thiazoline (2MT)

We assessed innate fear response to an ecologically relevant aversive stimulus, i.e. predator odor by means of used cat litter or a synthetic analog of a fox anogenital product (2-methyl-2-thiazoline; 2MT), in a transparent Plexiglass arena (43 × 27 × 19 cm). Testing was carried out in a fume hood with medium-light intensity (120 lux) in covered arenas

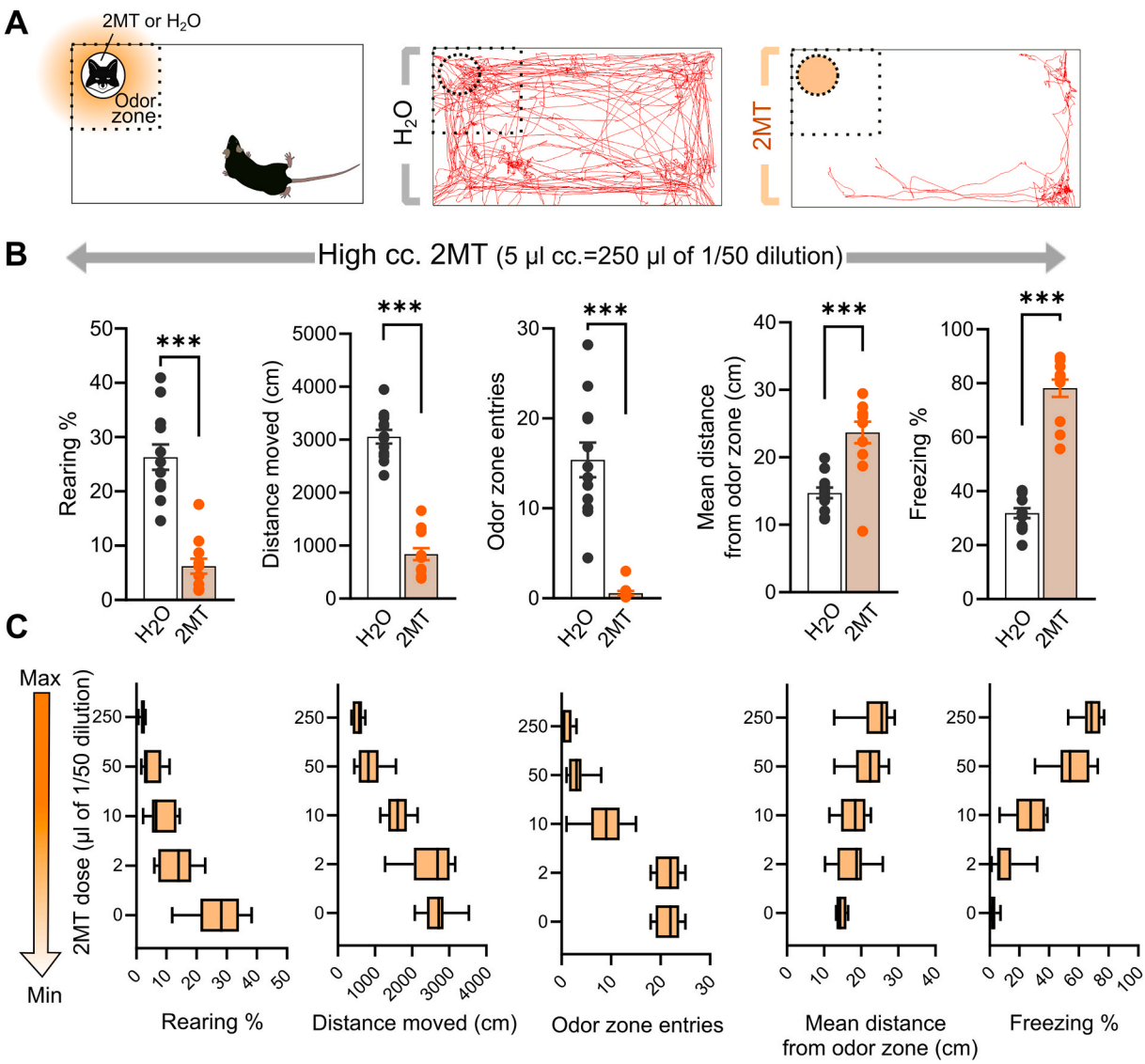

Fig. 1. 2MT elicits robust and dose-dependent innate fear responses in mice. (A) Left panel illustrates the testing apparatus. Dashed lines indicate the defined 'odor zone' containing a filter paper with H_2O (no odor) or 2MT. Right panel illustrates representative trajectory plots of individual mice exposed to H_2O or 2MT. (B) Innate fear response quantified by five behavioral variables on the active-passive defense dimension. 2MT induced a robust fear response indicated by reduced distance moved, less rearing and entries into the odor zone, as well as increased mean distance from the odor zone, and time spent with freezing (n = 12/group). (C) Dose-response curve of 2MT-induced fear. 2MT dose-dependently increased the innate fear response reflected by all variables. Box plots represent medians, minimum and maximum values (n = 8/group). Graph bars show means ± SEM. ***$p < 0.001$ (Student t-test).

to equalize odor exposure across subjects. Animals were habituated to the clean, empty arena for 10 min 24 h before testing to lower novelty stress. During testing, cat urine was presented using soiled cat litter in a perforated 50 ml conical tube affixed to the floor in the corner. 2MT (#M83406, Sigma Aldrich) was presented on a filter paper placed in a plastic vial cap affixed to the corner. We defined a 7 × 11 cm 'odor zone' around the odor source to quantify avoidance and exploration of predator odor (Fig. 1A). At start, animals were placed in the corner opposing the odor zone and were left to freely explore in the covered arena for 10 min. Filter papers were immediately removed at the end of the test, then the testing arena was cleaned with water, wiped dry, and left ventilated for additional 2 min before the next test. We used five behavioral variables to characterize the innate fear response in detail on the passive-active dimension: (1) locomotor/horizontal exploratory activity (total distance moved in cm), (2) vertical exploratory activity (time spent with rearings), (3) the number of entries/approaches into the odor zone, (4) mean distance from the odor zone (cm), and (5) time spent with immobility/freezing. All behavioral variables were quantified using EthoVision XT 15 software except rearing, which was hand-scored by an experimenter blind to treatment groups (Solomon Coder, Hungary; https://solomoncoder.com/).

2.6. Immunohistochemistry and image analysis

2.6.1. Tissue processing

Mice were anesthetized with a ketamine-xylazine solution (16.6 mg/ml and 0.6 mg/ml, respectively) and transcardially perfused with ice-cold phosphate-buffered saline (PBS), followed by ice-cold paraformaldehyde (PFA; 4% in PBS). Brains were rapidly removed and post-fixed overnight in 4% PFA at 4 °C, then incubated in a solution containing 30% sucrose in PBS before slicing. 30 μm coronal sections were collected on a sliding microtome and stored in a cryoprotectant solution (containing 20% glycerin, 30% ethylene glycol) at −20 °C until immunohistochemical staining.

2.6.2. Verification of virus extensions

We labeled mCherry by immunohistochemistry using primary antibody against red fluorescent protein (RFP) to verify virus expression in the BNST. Briefly, after several rinses in PBS, sections (90 μm apart) were incubated in PBS containing 0.3% Triton X-100 (TxT, Sigma-Aldrich) and 0.3% H_2O_2 for 30 min followed by 2% bovine serum albumin (BSA, Sigma-Aldrich) diluted in PBS for 1 h. Primary antibody solution (1:4000 rabbit anti-RFP, #600-401-379, Rockland, Limerick, PA, USA; diluted in PBS containing 2% BSA and 0.1% Triton-X) was left over on the slices for 2 days at 4 °C. After several rinsing with PBS, slices were incubated in biotin-conjugated donkey anti-rabbit secondary antibody (1:1000 in 2% BSA and PBS, #711-065-152, Jackson ImmunoResearch, Cambridgeshire, United Kingdom) for 2 h. Labeling was amplified by avidin-biotin complex (1:1000; Vector Laboratories, Burlingame, CA, USA) by incubation for 1 h at room temperature. The peroxidase reaction was developed in the presence of diaminobenzidine tetrahydrochloride (0.2 mg/ml), nickel–ammonium sulfate (0.1%), and hydrogen peroxide (0.003%) dissolved in Tris buffer. Sections were mounted onto gelatin-coated slides, dehydrated, and coverslipped with DPX Mountant (Sigma-Aldrich/Merck, Darmstadt, Germany). Regions of interest were digitalized by an Olympus DP70 Light Microscope and CCD camera system. All animals with virus extension outside of the BNST were excluded from the analysis (N = 2–9/group: N = 5–6 of control and N = 7–9 of hM4Di subjects in case of sst-ires-cre mice; N = 2–3 of control and N = 4–9 of hM4Di subjects in case of crh-ires-cre mice). Generally, mCherry-positive cell bodies were observed along the whole rostrocaudal axis of the BNST similar to our previous studies (Bruzsik et al., 2021).

2.6.3. C-Fos immunohistochemistry and microscopy

To verify that CNO treatment resulted in significant inhibition of DREADD-expressing neurons of the BNST, we labeled c-Fos immediate-early gene product to quantify the activity of hM4Di expressing neurons. Mice were perfused 90 min after behavioral testing (with CNO injection 40 min before testing). We used fluorescent immunolabeling against c-Fos and RFP as described above (1:2000 guinea-pig polyclonal anti-c-Fos IgG, #226004, Synaptic Systems with monoclonal rabbit anti-RFP IgG 1:1000, #600-401-379, Rockland), which were detected by fluorescent-conjugated antibodies (1:500 Cy3 conjugated donkey anti-rabbit, #134845, Jackson ImmunoResearch, and 1:500 Alexa-488 conjugated donkey anti-guinea-pig, #S32354, ThermoFisher Scientific, Waltham, MA, USA). Fluorescent labeling was imaged using either C2 Confocal Laser-Scanning Microscope (CFI Plan Apo VC20X/N.A. 0.75, xy: 0.62 μm/pixel, Nikon Europe, Amsterdam, The Netherlands), or Panoramic Digital Slide Scanner (Zeiss, Plan-Apochromat 10X/NA 0.45, xy: 0.65 μm/pixel, Panoramic MIDI II; 3DHISTECH, Budapest, Hungary) equipped with LED (Lumencor, SPECTRA X light engine). RFP/c-Fos co-expression was counted manually in 3 brain sections exhibiting the highest density of RFP + expression using standardized settings (contrast, intensity) across subjects. For statistical analysis, we calculated the percentage of c-Fos+/RFP + cell number compared to total RFP + cell number.

2.7. Statistics

Data are expressed as mean ± standard error of the mean (SEM). Differences between groups were analyzed using Statistica software 13.5 (Tibco, Palo Alto, CA, USA) by means of Student's t-test, or Mann-Whitney *U* test when requirements for t-tests were not fulfilled. In 2MT dose-response experiment, we used repeated measure ANOVA, followed by Tukey's post hoc analyses. The significance level was set at $p < 0.05$ throughout, all p values are indicated with exact numbers.

3. Results

3.1. Establishing a scalable innate fear paradigm using synthetic predator odor component 2-methyl-2-thiazoline (2MT)

First, we exposed adult male C57BL/6J mice to either H_2O or undiluted 2MT (5 μl) to validate the fear-inducing capacity of 2MT and characterize the defensive behavioral repertoire with multiple variables. All behavioral variables indicated robust fear reaction in the presence of 2MT: decreased locomotor activity/exploration (i.e. distance moved: $t = -12.911$, $p < 0.001$), decreased rearing ($t = -7.432$, $p < 0.001$), less approach to the odor source ($t = -7.805$, $p < 0.001$), higher mean distance from the odor source ($t = 5.027$, $p < 0.001$), and increased time of freezing ($t = 12.563$, $p < 0.001$) (Fig. 1A and B).

Next, we assessed the dose-response curve of 2MT to define and optimize low and high stimuli for chemogenetic manipulations, i.e. reliable fear response with differential characteristics of active-passive responses; and provide a range for bidirectional manipulations. We tested four decreasing doses on a nearly logarithmic scale, i.e. from 250 μl (equivalent with the undiluted dose used above) to 1/125 dose (250, 50, 10, 2 μl of a 50x dilution of 2MT). We observed a dose-dependent response curve (Fig. 1C): increasing locomotor activity/exploration ($F(1,35) = 43.41$, $p < 0.001$), increasing rearing/risk assessment ($F(1,35) = 29.52$, $p < 0.001$), more entries to the odor zone ($F(1,35) = 40.19$, $p < 0.001$), reduced mean distance from the odor source ($F(1,35) = 6.21$, $p < 0.001$), and reduced time of freezing ($F(1,35) = 67.90$, $p < 0.001$) by the gradual decrease of the 2MT dose. Considering that 2 μl dose was ineffective (Tukey's posthoc for all variables: $p > 0.54$; except decreased approach: $p = 0.025$), and 50 μl dose resulted in a similar behavioral outcome as 250 μl dose (Tukey's posthoc for all variables: $p > 0.52$; except somewhat lower freezing levels, $p = 0.072$), we selected 10 μl and 250 μl doses for further experiments as low and high stimulus intensities (accordingly we refer to them as 'low- and high-dose' throughout the manuscript). These two doses were effective inducer of the fear response

indicated by all variables (Tukey's posthoc for all variables of both doses: $p < 0.001$, except mean distance from the odor source for 10 μl dose: $p = 0.57$), but they also evoked a markedly different level of fear response (Tukey's posthoc for all variables: $0.001 < p < 0.05$).

3.2. Chemogenetic inhibition of $BNST^{SST}$ neurons reduces innate fear response under weak threat

To selectively test how neurochemically distinct neuronal populations of the BNST modulate innate fear responses elicited by weak and strong (i.e. uncertain and more imminent) threats, we applied cell-type specific chemogenetic inhibition of $BNST^{SST}$ neurons during 2MT exposures using sst-ires-cre mice (n = 9–10/groups) (Fig. 2A, C, and D). On the behavioral level, chemogenetic inhibition of $BNST^{SST}$ neurons significantly reduced fear responses evoked by low-dose 2MT, indicated by all variables except freezing (Fig. 2C and D, distance moved: $t = -2.203$, $p = 0.041$; entries into the odor zone: $t = -2.348$, $p = 0.031$; rearing: $t = -2.392$, $p = 0.029$; mean distance from the odor zone: $t = 3.203$, $p = 0.005$; freezing: $t = 1.436$, $p = 0.168$; n = 9–11/group). Importantly, none of these variables were changed when chemogenetic inhibition was applied in an open field arena without 2MT exposure (Fig. 2B; center time%: $t = -0.741$, $p = 0.468$; distance moved: $t = -0.506$, $p = 0.619$; rearing: $t = 0.140$, $p = 0.890$; freezing: $t = 0.201$, $p = 0.843$; n = 9–10/group). Noteworthy, also freezing is significantly decreased ($p = 0.034$) if one considers the highest individual value as an outlier within the hM4Di group (2.12 SD above the mean), suggesting that chemogenetic inhibition effect was reflected by all behavioral variables. We also confirmed the marked reduction of neuronal activity of hM4Di-expressing neurons during low-dose 2MT exposure (40 min after CNO injection) indicated by decreased number of c-Fos + cells compared to subjects expressing control fluorophores without hM4Di (n = 6, $t = 5.165$, $p < 0.001$), although this reduction of neuronal activity was not reflected quantitatively in behavioral alterations, i.e. no significant correlation between c-Fos numbers and behavioral variables ($p > 0.191$) (Fig. 2E and F). In contrast, chemogenetic inhibition had no effect on high dose (250 μl of 1/50 dilution) 2MT evoked fear responses (distance moved, $t = 0.039$, $p = 0.969$; entries into the odor zone: $t = 0.244$, $p = 0.808$; mean distances from the odor zone: $t = -0.078$, $p = 0.938$; rearing: $t = 1.639$, $p = 0.114$; freezing: $t = -0.671$, $p = 0.508$; n = 9–11/group) (Fig. 2G).

3.3. Chemogenetic inhibition of $BNST^{CRH}$ neurons has no impact on innate fear response evoked by 2MT

Next, we tested the impact of chemogenetic inhibition of $BNST^{CRH}$ neurons on the same innate fear response evoked by low- and high-dose 2MT exposure using crh-ires-cre mice (n = 9–15/group) (Fig. 3A, C and D). In contrast to $BNST^{SST}$ manipulation, chemogenetic inhibition of $BNST^{CRH}$ neurons had no effect on the fear response evoked by low-dose 2MT as indicated by unaltered distance moved ($t = 0.710$, $p = 0.484$), entries into the odor zone ($t = -0.884$, $p = 0.386$), time spent with rearing ($t = 0.643$, $p = 0.526$), freezing ($t = -0.399$, $p = 0.693$), and mean distance from the odor zone ($t = -0.418$, $p = 0.679$) (Fig. 3C). Similarly, high-dose 2MT evoked fear response was not altered (Fig. 3D): total distance travelled ($t = -1.805$, $p = 0.084$), entries into the odor zone ($t = 0.894$, $p = 0.380$), rearing ($t = -1.086$, $p = 0.288$), freezing ($t = 1.600$, $p = 0.123$), and mean distance from the odor zone ($t = 0.264$, $p = 0.793$; n = 11–14/groups). None of these variables were changed when chemogenetic inhibition was applied in an open field arena without 2MT exposure (Fig. 3B; center time%: $t = 0.217$, $p = 0.829$; distance moved: $t = -1.400$, $p = 0.175$; rearing: $t = -0.297$, $p = 0.768$; freezing: $t = 1.636$, $p = 0.116$; n = 8–16/group).

3.4. Chemogenetic inhibition of $BNST^{CRH}$ neurons enhances the innate fear response evoked by cat odor

To resolve contradiction between our results, i.e. inability to modulate 2MT-induced fear by $BNST^{CRH}$ inhibition, and previous findings showing significant CRH + neuronal activation evoked by predator odor or TMT exposure (Butler et al., 2016; Giardino et al., 2018), we further explored $BNST^{CRH}$ manipulation using a different predator stimulus. Since previous reports showed that the CRH system of the central amygdala is recruited by weak threats only (i.e. low-intensity footshocks, (Sanford et al., 2017), we tested if manipulation of $BNST^{CRH}$ neurons is effective under lower threat conditions. Noteworthy, even low-dose of 2MT is a potent fear-eliciting agent resulting in ~30% of test time spent with freezing, and marked avoidance of the odor zone (3–4 entries/10 min) in control mice (Fig. 3C), which could prevent 'low threat' effects when CRH neurons are engaged, despite our effort to define a minimal dose of 2MT for our first experiments. Previously, we found that cat urine is a mild stressor for mice eliciting low, but detectable, levels of freezing and avoidance. Accordingly, first we confirmed this effect in naïve adult male C57BL/6J mice (Fig. 4A and B). We observed significantly reduced locomotor activity ($t = 3.183$, $p = 0.003$) and increased time of freezing ($t = -2.790$, $p = 0.008$), without affecting entries into the odor zone ($t = 1.126$, $p = 0.216$), rearings ($t = 0.296$, $p = 0.768$), and mean distance from the odor zone ($t = -0.237$, $p = 0.813$) in mice exposed to soiled cat litter compared to clean litter material.

Next, we replicated our 2MT experiment with the same experimental settings, but we used cat urine as a threat stimulus (Fig. 4C and D). Chemogenetic inhibition of $BNST^{CRH}$ neurons resulted in enhanced fear response reflected by all variables: reduced distance moved ($t = 4.167$, $p < 0.001$), rearings (4.965, $p < 0.001$), entries into the odor zone ($t = 1.820$, $p = 0.08$), as well as higher mean distance from the cat odor ($t = -2.696$, $p = 0.015$) and freezing levels ($t = -2.648$, $p = 0.017$) (n = 8–10/groups) (Fig. 4D). The effect of chemogenetic inhibition on BNST activity was also detectable on the neuronal level indicated by reduced c-Fos expression in $BNST^{CRH}$ cells (n = 8–10/groups), although again this reduction of neuronal activity was not reflected quantitatively in behavioral alterations, i.e. no significant correlation between c-Fos numbers and behavioral variables ($p > 0.120$) (Fig. 4E and F).

In contrast to $BNST^{CRH}$ neurons, chemogenetic inhibition of $BNST^{SST}$ neurons resulted in no alteration of any behavioral variables during cat odor exposure: distance moved ($t = 0.239$, $p < 0.813$), rearings ($t = -0.636$, $p < 0.534$), entries into the odor zone ($t = -1.246$, $p = 0.231$), mean distance from cat odor ($t = 0.180$, $p = 0.859$) and freezing levels ($t = 0.010$, $p = 0.992$) (n = 8–9/groups) (Fig. 4G).

4. Discussion

Here, we report that chemogenetic inhibition of neurochemically distinct BNST neurons bidirectionally shifted innate fear responses evoked by predator odor stimuli. Namely, inhibition of $BNST^{SST}$ neurons resulted in reduced fear indicated by enhanced exploratory activity and lowered avoidance of predator odor 2MT, whereas inhibition of $BNST^{CRH}$ neurons enhanced fear indicated by decreased exploratory activity, increased freezing and avoidance of cat odor. Importantly, chemogenetic manipulations of BNST were effective only under weak threat conditions, i.e. exposure to low dose of 2MT or less aversive cat odor, which presumably represented less imminent threats.

The various fear-inducing potential of distinct predator odors has been well-documented, but so far few studies have investigated how stimulus and threat intensity shapes the fear response to the same predator (Perez-Gomez et al., 2015; Takahashi et al., 2005; Wallace and Rosen, 2000). Here, we established a dose-dependent fear response paradigm by means of 2MT exposure: higher doses gradually decreased exploratory activity and rearing, increased avoidance, and precipitated significant freezing, supposedly correlating with threat imminence.

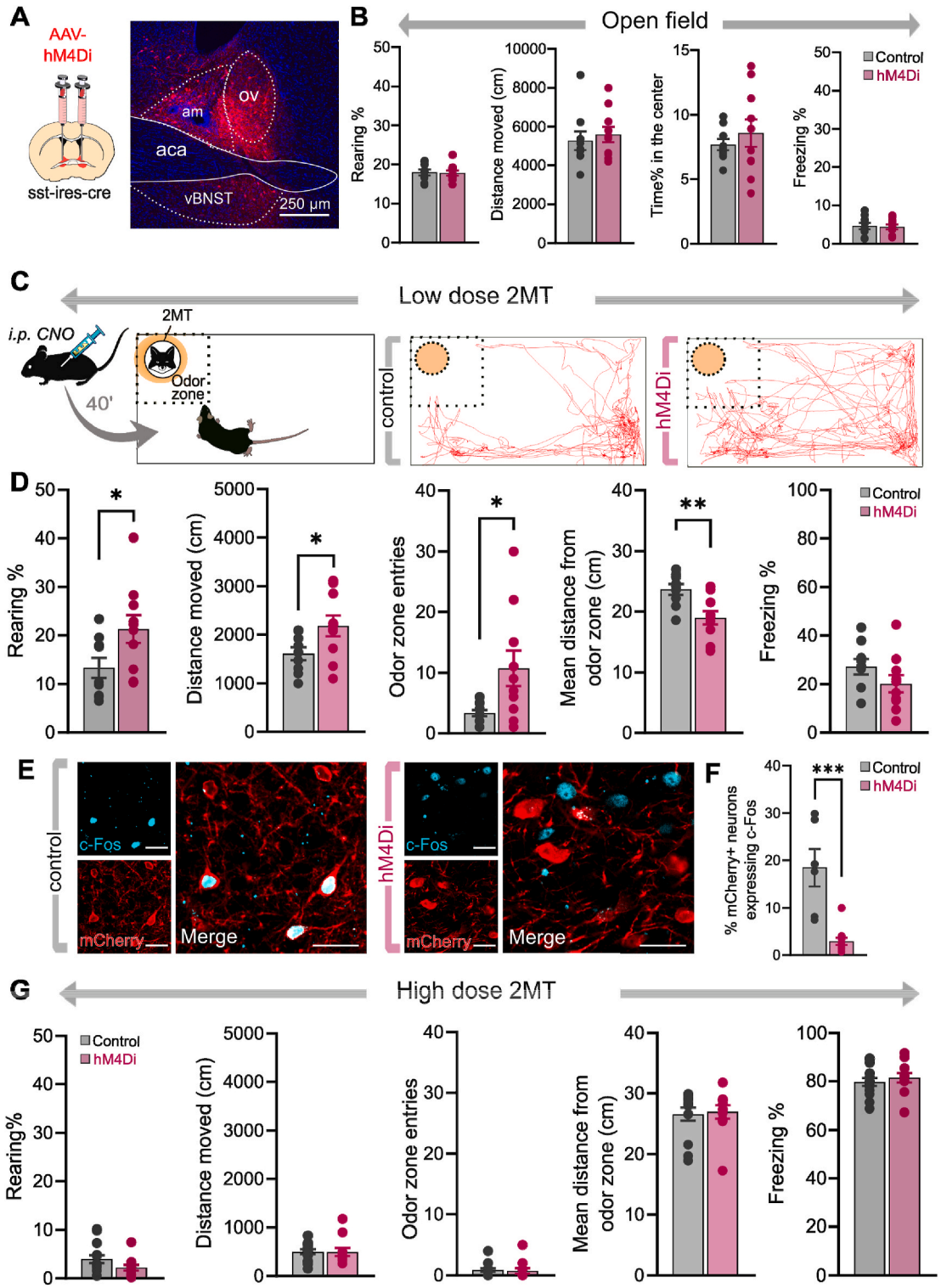

Fig. 2. Chemogenetic inhibition of BNST^{SST} neurons reduces fear response under weak threat. (A) Schematics of stereotaxic delivery of AAVs encoding hM4Di inhibitory DREADD receptors or control fluorophore in sst-ires-cre mice, and representative photomicrograph illustrating hM4Di-mCherry expression 4–6 weeks later. (B) Exploratory and anxiety-like behaviors in an open field arena were not altered by chemogenetic inhibition of BNST^{SST} neurons. (C) Illustration of experimental settings and representative trajectory plots of individual 2MT-exposed mice expressing control fluorophore or hM4Di receptors. (D) Innate fear responses during low-dose 2MT exposure were blunted by chemogenetic inhibition of BNST^{SST} neurons. (E) Representative confocal microscopic images of c-Fos expression in the BNST from 2MT-exposed mice expressing control fluorophore or hM4Di receptors (40 min after CNO injection). (F) hM4Di-expressing neurons exhibited reduced neuronal activity during 2MT-exposure compared to controls indicated by decreased cFos+/mCherry + co-labeling. Scale bars represent 25 µm. (G) Chemogenetic inhibition had no effect on fear responses in case of high dose of 2MT exposure. Data are expressed as means ± SEM. *$p < 0.05$, **$p < 0.01$ (Student t-test), ***$p < 0.001$ (Mann-Whitney test). *Abbreviations: aca: anterior commissure, am: anteromedial BNST, ov: oval nucleus of BNST, vBNST: ventral BNST.*

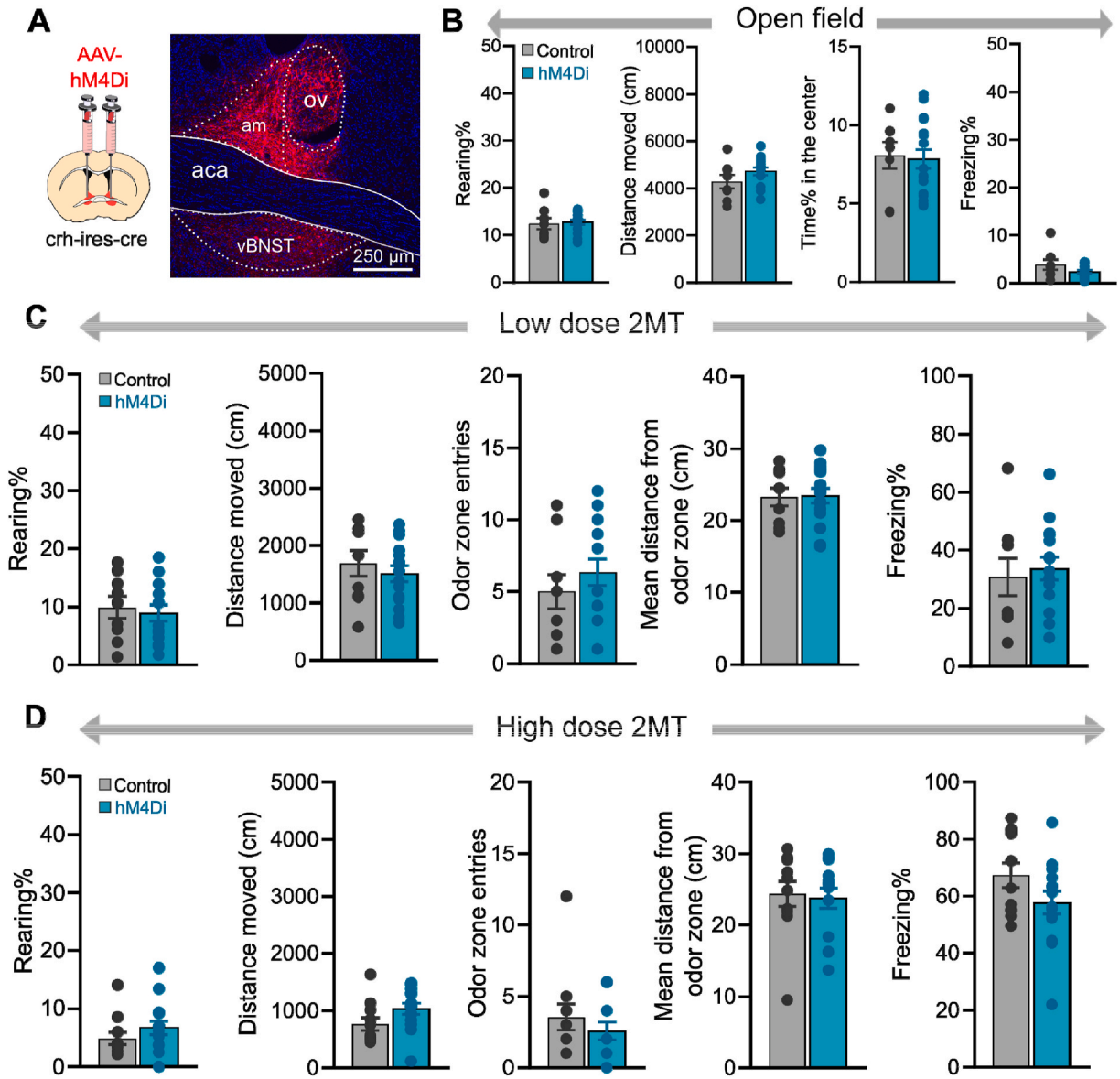

Fig. 3. Chemogenetic inhibition of BNST^{CRH} neurons has no impact on innate fear response evoked by 2MT. (A) Schematics of stereotaxic delivery of AAVs encoding hM4Di inhibitory DREADD receptors or control fluorophore in crh-ires-cre mice mice, and representative photomicrograph illustrating hM4Di-mCherry expression 4–6 weeks later. (B) Exploratory and anxiety-like behavior in an open field arena were not altered by chemogenetic inhibition of BNST^{CRH} neurons. (C and D) Innate fear responses during low- and high-dose 2MT exposure, respectively. Chemogenetic inhibition of BNST^{CRH} neurons had no effect on any behavioral variables of the fear response. Data are expressed as means ± SEM. *Abbreviations: aca: anterior commissure, am: anteromedial BNST, ov: oval nucleus of BNST, vBNST: ventral BNST.*

Since predatory odor stimuli represent spatio-temporal information about potential danger (Apfelbach et al., 2015), fear response elicited by low and high dose of 2MT likely represents an adaptive coping corresponding with threat proximity (i.e. shift from active exploration towards avoidance and immobility when threat is imminent and escape becomes risky). In line with this, previous papers showed that rats exhibit differential fear responses for proximal and remote danger cues (Andraka et al., 2021; Hegab et al., 2014). Here, we showed that 2MT provides a feasible method to control predator odor threat in order to manipulate danger signals, which can be applied by future studies aiming to scale threat intensities (e.g. in PTSD models, where a major validity criterion is the correlation between stress intensity and PTSD-like sequelae (Yehuda and Antelman, 1993).

In the last decades, significant work explored specific amygdalar circuits regulating different aspects of acute and learned fear responses (Herry and Johansen, 2014; Tovote et al., 2015a). In contrast, the BNST gained significant attention only recently, partly due to the growing number of human imaging studies indicating that negative valence stimuli activate the BNST with additional hyperactivation in subjects with anxiety and trauma-related disorders (Brinkmann et al., 2017; Buff et al., 2017; Somerville et al., 2010). More specifically, imaging data in challenging situations pointed out that uncertain threats are particularly evocative for BNST activity, e.g. during anticipation of aversive stimuli, or exposure to ambiguous, less predictable threats (Herrmann et al., 2016; Mobbs et al., 2010; Naaz et al., 2019). Observations from animal models confirmed that low predictability and uncertainty are crucial factors in the engagement of BNST circuits (Goode et al., 2020; Goode and Maren, 2017), which refined previous models on extended amygdala functions (i.e. amygdala vs BNST functional division) by extending 'phasic vs sustained fear' functional divisions with dimensions of threat predictability and valence monitoring (Davis et al., 2010; Lebow and Chen, 2016; Shackman and Fox, 2016). In this respect,

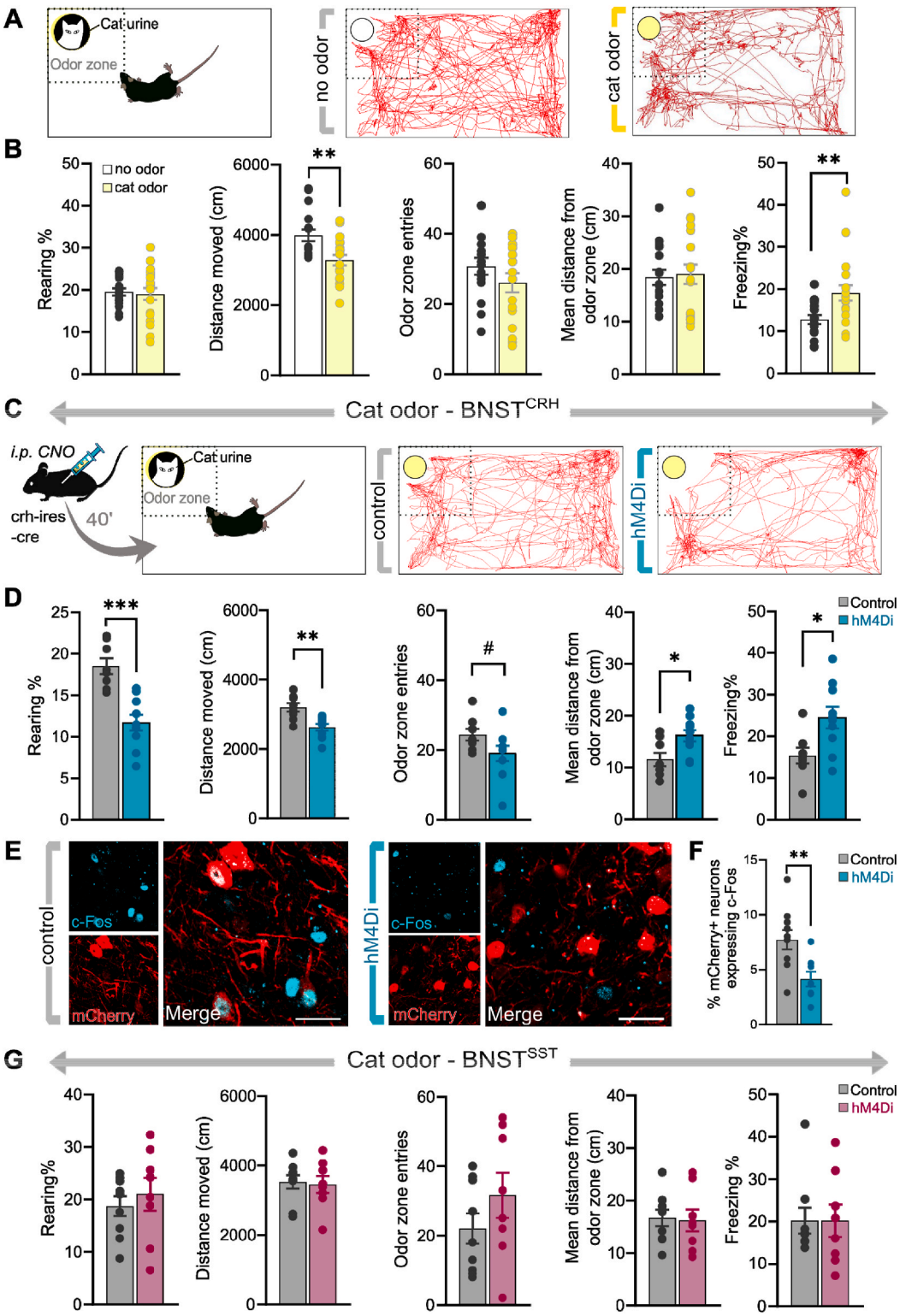

Fig. 4. Chemogenetic inhibition of BNST^{CRH} neurons enhances innate fear response evoked by cat odor. (A) Illustration of experimental settings and representative trajectory plots of individual mice exposed to clean or soiled cat litter. (B) Assessment of the behavioral profile of mice exposed to cat odor. Cat odor exposure significantly decreased locomotor activity and increased freezing behavior (n = 16–19/group), without altering approaches, rearing, or mean distance from the odor zone. (C) Illustration of experimental settings and representative trajectory plots of individual cat odor exposed mice expressing control fluorophore or hM4Di receptors. (D) Inhibition of BNST^{CRH} neurons resulted in enhanced fear response indicated by all behavioral variables (n = 8–10/group). (E) Representative confocal microscopic images of the BNST from cat odor exposed mice expressing control fluorophore or hM4Di receptors (40 min after CNO injection). (F) hM4Di-expressing neurons exhibited reduced neuronal activity during cat odor exposure compared to controls indicated by decreased cFos+/mCherry + co-labeling (n = 6–8/group). (G) Inhibition of BNST^{SST} neurons had no impact on the fear response indicated by all behavioral variables (n = 8–9/group). Data are expressed as means ± SEM. *$p < 0.05$, **$p < 0.01$, #p = 0.08 (Student t-test).

threat-monitoring BNST circuits can be significant contributors to generalized and exaggerated anxiety-like states (Avery et al., 2016).

Our findings support that the dimension of stimulus intensity as a predictor of threat probability is a crucial factor in the recruitment of BNST circuits. Even robust chemogenetic inhibition of SST or CRH neuronal activity (down to ~15% and ~50% activity, respectively, compared to controls) had no effect on any form of the fear response, when 2MT predator stimulus was intense. In contrast, when we lowered stimulus intensity significantly, BNST inhibition became apparent in a reduced fear response in the case of SST neurons. Noteworthy, our effects seem to be specific to predatory threat since the same manipulation was ineffective in an open field arena, which also confirmed that general locomotor and exploratory activity is not affected. This conclusion is also supported by previous studies reporting minimal or no effect of chemogenetic manipulation of BNST on anxiety-like behavior and exploratory activity in the elevated plus-maze and open field tests without additional stressors (Marcinkiewcz et al., 2016; Mazzone et al., 2018). Interestingly, a comparative approach in rats pointed out that stressors and level of anxiety can be crucial in the outcome: chemogenetic inhibition of CeA^{CRH} neurons was an effective anxiolytic manipulation only if a previous stressor was applied in order to increase anxiety level (Pomrenze et al., 2019), suggesting again that the level of threat and stress is a crucial factor how CRH and other circuits of the extended amygdala are activated. Our findings on cell type specificity are consistent with previous studies reporting that SST neurons drive passive fear response and coping in different contexts across multiple brain regions (Cummings and Clem, 2020; Philip Tovote et al., 2015; Yu et al., 2016), and increase anxiety-like avoidance behavior (Ahrens et al., 2018). Recently, we also showed that hyperactivity of $BNST^{SST}$ neurons enhance fear consolidation, and subsequent freezing during fear recalls in a safe context without affecting the acute fear response when strong aversive (i.e. footshock) stimuli are present in a predictable way (Bruzsik et al., 2021). Together these results support the notion that $BNST^{SST}$ neurons promote passive fear responses to low intensity/uncertain threats, which can be a complementary function to central amygdala (CeA) circuits, where CeA^{SST} neurons are engaged under imminent threat conditions and drive passive fear response to direct/-strong threats, including a high dose of 2MT (Andraka et al., 2021; Isosaka et al., 2015; K. Yu et al., 2016). Importantly, the lack of impact of $BNST^{SST}$ inhibition under cat odor exposure points out that further characteristics and dimensions of threatening stimuli may be important. For instance, we can hypothesize that $BNST^{SST}$ neurons were not activated by even weaker threat such as cat odor, or olfactory pathways can be divergent and target BNST cell populations differentially.

In contrast to $BNST^{SST}$, inhibition of $BNST^{CRH}$ neurons had no effect under the same condition, i.e. low dose 2MT exposure. Considering that CeA^{CRH} neurons regulate fear learning of low, but not strong, intensity stimuli (Sanford et al., 2017), we hypothesized that even low dose 2MT may represent a threat condition, where CRH circuits are not engaged or masked/compensated by other (e.g. amygdala) circuits or by their downstream effects. Therefore, we turned to another predator stimulus, i.e. soiled cat litter representing a stimulus intensity from a natural setting, to lower further threat intensity/certainty. As we showed, cat litter evoked a much weaker fear response: exploratory activity was increased to ~200%, freezing was reduced to ~50%, and mice entered the odor zone 4–5 times more compared to low dose 2MT exposure, which is similar to previous findings comparing the effects of urinal-fecal stimuli and synthetic component TMT (Buron et al., 2007; Hacquemand et al., 2013). Noteworthy, cat litter was still able to evoke a significant, detectable fear response compared to clean litter-exposed controls, although with different response profile compared to 2MT (i.e. reducing general activity in conjunction with elicited freezing). Under this weak threat condition likely representing a natural situation, inhibition of $BNST^{CRH}$ resulted in enhanced fear responses, pointing out an opposite (i.e. anxiolytic or approach promoting) role of this cell population, compared to $BNST^{SST}$. Latter finding implies important functional similarity, as well as complementarity, of SST and CRH neurons across brain regions if one interprets our effects as shifts from passive to active responses as suggested previously (Daviu et al., 2020; Daviu and Bains, 2021; Fadok et al., 2017; Luchsinger et al., 2021), although we need to emphasize that our effects were more general shifts toward avoidance or approach with corresponding changes in activity and freezing. Consistency of cell type specific effects may open perspective for translational research if these specific neuronal populations exhibit specific receptor expression profiles that can be used for pharmacological manipulations.

On the other hand, our findings are also affirmative for functional similarities of CRH neurons across extended amygdala regions by showing the specific impact of $BNST^{CRH}$ neurons on responses evoked by weak threats, which corresponds with the engagement of CeA^{CRH} neurons by weak unconditioned stressors or social danger signals (Andraka et al., 2021; Sanford et al., 2017). Again, we cannot exclude the possibility that the qualitative nature of different predator odors was a confounding factor here, as it has been shown that chemically diverse kairomones can be processed in partially non-overlapping pathways (Perez-Gomez et al., 2015). Unfortunately, cat urine is not a purified, single-molecule compound; consequently, it was not suitable to apply in a dose-dependent manner to clarify stimulus strength issues more exactly. However, our negative finding on $BNST^{SST}$ manipulation, i.e. no impact on any behavioral variables during cat odor exposure, support the hypothesis that besides stimulus strength, the qualitative nature of aversive stimuli is a significant determinant which circuits of BNST is activated under threatening conditions. Another important limitation of our paradigm was the lack of active escape/flight response (sporadically occurring), although we characterized behavioral variables in detail. Considering the impact of CeA^{CRH} neurons on active flight response and rearing (Fadok et al., 2017), it is possible that our behavioral paradigm could not detect certain behavioral effects, although decreased rearing (highest effect size) following $BNST^{CRH}$ inhibition points to the same direction as CeA^{CRH} effect. Finally, a recent paper manipulating CeA^{CRH} neurons in a social observational fear paradigm also indicated the recruitment of CRH neurons by remote/less direct threats presented by conspecifics (Andraka et al., 2021), suggesting that neurochemically distinct neuronal populations of the extended amygdala can code specific features of aversive stimuli and shape adaptive responses accordingly.

Future studies with manipulations of distinct characteristics of aversive stimuli and specific neuronal populations of extended amygdala circuits will further advance our understanding of how negative valence is translated into specific adaptive and maladaptive actions. Additionally, future studies will need to test if the sexually dimorphic nature of the BNST is an important modulator of these effects, i.e. female mice may respond differently to BNST manipulations.

5. Conclusion

Taken together, our results suggest that $BNST^{SST}$ and $BNST^{CRH}$ neurons regulate innate fear responses to predatory threats in a complementary manner, but only when stimulus intensity is low, i.e. representing a rather uncertain, remote threat. This observation further supports the notion that the modulatory role of BNST in defensive behavior is highly dependent on threat imminence and predictability. Latter may also explain some clinical observations reporting hyperactivity of BNST in anxiety and trauma-related disorders, where several neutral/safe stimuli interpreted as potential threats eliciting exaggerated or context-inadequate fear responses. Our data suggest that hyperactive SST and/or hypoactive CRH system of the BNST can contribute to such an abnormal 'threat detector' system, and hence, can determine core features of these disorders.

CRediT authorship contribution statement

Biborka Bruzsik: Conceptualization, Methodology, Formal analysis,

Investigation, Writing – original draft, Writing – review & editing, Visualization. **Laszlo Biro:** Conceptualization, Investigation, Writing – review & editing. **Klara Rebeka Sarosdi:** Investigation, Resources. **Dora Zelena:** Investigation, Resources, Writing – review & editing. **Eszter Sipos:** Investigation, Resources. **Huba Szebik:** Investigation, Resources. **Bibiána Török:** Investigation, Resources. **Eva Mikics:** Conceptualization, Writing – review & editing, Supervision, Funding acquisition. **Mate Toth:** Conceptualization, Methodology, Formal analysis, Investigation, Writing – original draft, Writing – review & editing, Supervision, Funding acquisition.

Declaration of competing interest

The authors declare that they have no known competing financial interests or personal relationships that could have appeared to influence the work reported in this paper.

Data availability

Data will be made available on request.

Acknowledgments

This work was supported by National Research, Development and Innovation Office grant #FK129296 (for MT), and the Hungarian Brain Research Program grant #2017–1.2.1-NKP-2017-00002 (for EM). This work was also supported by New National Excellence Program of the Ministry for Innovation and Technology Grants #UNKP-18-3-III-SE-22 (for LB), #UNKP-19-2-I-ELTE-574 (for HS), and #UNKP-20-5-SE, #UNKP-21-5-SE-13 (for MT) from the source of the National Research, Development and Innovation Fund, and the Bolyai Janos Research Fellowship (for MT). We thank all the core facilities of our institute for their supportive help: the Behavioral Studies Unit for help with behavioral testing (Dr. Kornél Demeter), the Nikon Microscopy Center for help with microscopy (Dr. László Barna and Dr. Pál Vági), the Virus Technology Unit for help with viral surgeries, the Medical Gene Technology Unit for help with mouse lines. We also thank Beata Barsvari for technical assistance.

References

Ahrens, S., Wu, M.V., Furlan, A., Hwang, G.R., Paik, R., Li, H., Penzo, M.A., Tollkuhn, J., Li, B., 2018. A central extended amygdala circuit that modulates anxiety. J Neurosci 38, 5567–5583. https://doi.org/10.1523/JNEUROSCI.0705-18.2018.

Alheid, G.F., Heimer, L., 1988. New perspectives in basal forebrain organization of special relevance for neuropsychiatric disorders: the striatopallidal, amygdaloid, and corticopetal components of substantia innominata. Neuroscience 27, 1–39. https://doi.org/10.1016/0306-4522(88)90217-5.

Andraka, K., Kondrakiewicz, K., Rojek-Sito, K., Ziegart-Sadowska, K., Meyza, K., Nikolaev, T., Hamed, A., Kursa, M., Wojcik, M., Danielewski, K., Wiatrowska, M., Kublik, E., Bekisz, M., Lebitko, T., Duque, D., Jaworski, T., Madej, H., Konopka, W., Boguszewski, P.M., Knapska, E., 2021. Distinct circuits in rat central amygdala for defensive behaviors evoked by socially signaled imminent versus remote danger. Curr Biol 31, 2347–2358. https://doi.org/10.1016/j.cub.2021.03.047 e6.

Apfelbach, R., Blanchard, C.D., Blanchard, R.J., Hayes, R.A., McGregor, I.S., 2005. The effects of predator odors in mammalian prey species: a review of field and laboratory studies. Neurosci Biobehav Rev 29, 1123–1144. https://doi.org/10.1016/j.neubiorev.2005.05.005.

Apfelbach, R., Parsons, M.H., Soini, H.A., Novotny, M.V., 2015. Are single odorous components of a predator sufficient to elicit defensive behaviors in prey species? Front Neurosci 9, 263. https://doi.org/10.3389/fnins.2015.00263.

Asok, A., Ayers, L.W., Awoyemi, B., Schulkin, J., Rosen, J.B., 2013. Immediate early gene and neuropeptide expression following exposure to the predator odor 2,5-dihydro-2,4,5-trimethylthiazoline (TMT). Behav Brain Res 248, 85–93. https://doi.org/10.1016/j.bbr.2013.03.047.

Avery, S.N., Clauss, J.A., Blackford, J.U., 2016. The human BNST: functional role in anxiety and addiction. Neuropsychopharmacology 41, 126–141. https://doi.org/10.1038/npp.2015.185.

Bach, D.R., Guitart-Masip, M., Packard, P.A., Miro, J., Falip, M., Fuentemilla, L., Dolan, R.J., 2014. Human hippocampus arbitrates approach-avoidance conflict. Curr Biol 24, 541–547. https://doi.org/10.1016/j.cub.2014.01.046.

Brinkmann, L., Buff, C., Feldker, K., Tupak, S.V., Becker, M.P.I., Herrmann, M.J., Straube, T., 2017. Distinct phasic and sustained brain responses and connectivity of amygdala and bed nucleus of the stria terminalis during threat anticipation in panic disorder. Psychol. Med. https://doi.org/10.1017/S0033291717001192.

Bruzsik, B., Biro, L., Zelena, D., Sipos, E., Szebik, H., Sarosdi, K.R., Horvath, O., Farkas, I., Csillag, V., Finszter, C.K., Mikics, E., Toth, M., 2021. Somatostatin neurons of the bed nucleus of stria terminalis enhance associative fear memory consolidation in mice. J Neurosci 41, 1982–1995. https://doi.org/10.1523/JNEUROSCI.1944-20.2020.

Buff, C., Brinkmann, L., Bruchmann, M., Becker, M.P.I., Tupak, S., Herrmann, M.J., Straube, T., 2017. Activity alterations in the bed nucleus of the stria terminalis and amygdala during threat anticipation in generalized anxiety disorder. Soc Cogn Affect Neurosci 12, 1766–1774. https://doi.org/10.1093/scan/nsx103.

Buron, G., Hacquemand, R., Pourie, G., Lucarz, A., Jacquot, L., Brand, G., 2007. Comparative behavioral effects between synthetic 2,4,5-trimethylthiazoline (TMT) and the odor of natural fox (Vulpes vulpes) feces in mice. Behav Neurosci 121, 1063–1072. https://doi.org/10.1037/0735-7044.121.5.1063.

Butler, R.K., Oliver, E.M., Sharko, A.C., Parilla-Carrero, J., Kaigler, K.F., Fadel, J.R., Wilson, M.A., 2016. Activation of corticotropin releasing factor-containing neurons in the rat central amygdala and bed nucleus of the stria terminalis following exposure to two different anxiogenic stressors. Behav. Brain Res. 304, 92–101. https://doi.org/10.1016/j.bbr.2016.01.051.

Cohen, H., Kozlovsky, N., Matar, M.A., Zohar, J., Kaplan, Z., 2014. Distinctive hippocampal and amygdalar cytoarchitectural changes underlie specific patterns of behavioral disruption following stress exposure in an animal model of PTSD. Eur. Neuropsychopharmacol. 24, 1925–1944. https://doi.org/10.1016/j.euroneuro.2014.09.009.

Cruz, A., Heinemans, M., Marquez, C., Moita, M.A., 2020. Freezing displayed by others is a learned cue of danger resulting from Co-experiencing own freezing and shock. Curr Biol 30, 1128–1135. https://doi.org/10.1016/j.cub.2020.01.025 e6.

Cullinan, W.E., Herman, J.P., Watson, S.J., 1993. Ventral subicular interaction with the hypothalamic paraventricular nucleus: evidence for a relay in the bed nucleus of the stria terminalis. J. Comp. Neurol. 332, 1–20. https://doi.org/10.1002/cne.903320102.

Cummings, K.A., Clem, R.L., 2020. Prefrontal somatostatin interneurons encode fear memory. Nat Neurosci 23, 61–74. https://doi.org/10.1038/s41593-019-0552-7.

Daniel, S.E., Rainnie, D.G., 2016. Stress modulation of opposing circuits in the bed nucleus of the stria terminalis. Neuropsychopharmacology. https://doi.org/10.1038/npp.2015.178.

Davis, M., Walker, D.L., Miles, L., Grillon, C., 2010. Phasic vs sustained fear in rats and humans: role of the extended amygdala in fear vs anxiety. Neuropsychopharmacology 35, 105–135. https://doi.org/10.1038/npp.2009.109.

Daviu, N., Bains, J.S., 2021. Should I stay or should I go? CRHPVN neurons gate state transitions in stress-related behaviors. Endocrinology 162. https://doi.org/10.1210/endocr/bqab061.

Daviu, N., Fuzesi, T., Rosenegger, D.G., Rasiah, N.P., Sterley, T.L., Peringod, G., Bains, J. S., 2020. Paraventricular nucleus CRH neurons encode stress controllability and regulate defensive behavior selection. Nat Neurosci 23, 398–410. https://doi.org/10.1038/s41593-020-0591-0.

Day, H.E.W., Masini, C.V., Campeau, S., 2004. The pattern of brain c-fos mRNA induced by a component of fox odor, 2,5-dihydro-2,4,5-Trimethylthiazoline (TMT), in rats, suggests both systemic and processive stress characteristics. Brain Res. https://doi.org/10.1016/j.brainres.2004.07.079.

Deslauriers, J., Toth, M., Der-Avakian, A., Risbrough, V.B., 2018. Current status of animal models of posttraumatic stress disorder: behavioral and biological phenotypes, and future challenges in improving translation. Biol. Psychiatry 83, 895–907. https://doi.org/10.1016/j.biopsych.2017.11.019.

Fadok, J.P., Krabbe, S., Markovic, M., Courtin, J., Xu, C., Massi, L., Botta, P., Bylund, K., Muller, C., Kovacevic, A., Tovote, P., Luthi, A., 2017. A competitive inhibitory circuit for selection of active and passive fear responses. Nature 542, 96–100. https://doi.org/10.1038/nature21047.

Fanselow, M.S., Lester, L.S., 1988. A functional behavioristic approach to aversively motivated behavior: predatory imminence as a determinant of the topography of defensive behavior. In: Evolution and Learning. Lawrence Erlbaum Associates, Inc, Hillsdale, NJ, US, pp. 185–212.

Fendt, M., Endres, T., Apfelbach, R., 2002. Temporary Inactivation of the Bed Nucleus of the Stria Terminalis but Not of the Amygdala Blocks Freezing Induced by Trimethylthiazoline, a Component of Fox Feces.

Fung, B.J., Qi, S., Hassabis, D., Daw, N., Mobbs, D., 2019. Slow escape decisions are swayed by trait anxiety. Nat Hum Behav 3, 702–708. https://doi.org/10.1038/s41562-019-0595-5.

Giardino, W.J., Eban-Rothschild, A., Christoffel, D.J., Li, S.-B., Malenka, R.C., de Lecea, L., 2018. Parallel circuits from the bed nuclei of stria terminalis to the lateral hypothalamus drive opposing emotional states. Nat. Neurosci. https://doi.org/10.1038/s41593-018-0198-x.

Goode, T.D., Acca, G.M., Maren, S., 2020. Threat imminence dictates the role of the bed nucleus of the stria terminalis in contextual fear. Neurobiol Learn Mem 167, 107116. https://doi.org/10.1016/j.nlm.2019.107116.

Goode, T.D., Maren, S., 2017. Role of the bed nucleus of the stria terminalis in aversive learning and memory. Learn. Mem. https://doi.org/10.1101/lm.044206.116.

Goode, T.D., Ressler, R.L., Acca, G.M., Miles, O.W., Maren, S., 2019. Bed nucleus of the stria terminalis regulates fear to unpredictable threat signals. Elife 8. https://doi.org/10.7554/eLife.46525.

Gungor, N.Z., Pare, D., 2016. Functional heterogeneity in the bed nucleus of the stria terminalis. J. Neurosci. https://doi.org/10.1523/JNEUROSCI.0856-16.2016.

Hacquemand, R., Choffat, N., Jacquot, L., Brand, G., 2013. Comparison between low doses of TMT and cat odor exposure in anxiety- and fear-related behaviors in mice. Behav Brain Res 238, 227–231. https://doi.org/10.1016/j.bbr.2012.10.014.

Hartley, N.D., Gaulden, A.D., Baldi, R., Winters, N.D., Salimando, G.J., Rosas-Vidal, L.E., Jameson, A., Winder, D.G., Patel, S., 2019. Dynamic remodeling of a basolateral-to-central amygdala glutamatergic circuit across fear states. Nat Neurosci 22. https://doi.org/10.1038/s41593-019-0528-7, 2000–2012.

Hegab, I.M., Jin, Y., Ye, M., Wang, A., Yin, B., Yang, S., Wei, W., 2014. Defensive responses of Brandt's voles (Lasiopodomys brandtii) to stored cat feces. Physiol Behav 123, 193–199. https://doi.org/10.1016/j.physbeh.2013.10.030.

Herrmann, M.J., Boehme, S., Becker, M.P., Tupak, S.V., Guhn, A., Schmidt, B., Brinkmann, L., Straube, T., 2016. Phasic and sustained brain responses in the amygdala and the bed nucleus of the stria terminalis during threat anticipation. Hum Brain Mapp 37, 1091–1102. https://doi.org/10.1002/hbm.23088.

Herry, C., Johansen, J.P., 2014. Encoding of fear learning and memory in distributed neuronal circuits. Nat Neurosci 17, 1644–1654. https://doi.org/10.1038/nn.3869.

Isosaka, T., Matsuo, T., Yamaguchi, T., Funabiki, K., Nakanishi, S., Kobayakawa, R., Kobayakawa, K., 2015. Htr2a-Expressing cells in the central amygdala control the hierarchy between innate and learned fear. Cell 163, 1153–1164. https://doi.org/10.1016/j.cell.2015.10.047.

Janitzky, K., D'Hanis, W., Krober, A., Schwegler, H., 2015. TMT predator odor activated neural circuit in C57BL/6J mice indicates TMT-stress as a suitable model for uncontrollable intense stress. Brain Res 1599, 1–8. https://doi.org/10.1016/j.brainres.2014.12.030.

Klumpers, F., Kroes, M.C.W., Baas, J.M.P., Fernandez, G., 2017. How human amygdala and bed nucleus of the stria terminalis may drive distinct defensive responses. J Neurosci 37, 9645–9656. https://doi.org/10.1523/JNEUROSCI.3830-16.2017.

Kobayakawa, K., Kobayakawa, R., Matsumoto, H., Oka, Y., Imai, T., Ikawa, M., Okabe, M., Ikeda, T., Itohara, S., Kikusui, T., Mori, K., Sakano, H., 2007. Innate versus learned odour processing in the mouse olfactory bulb. Nature 450, 503–508. https://doi.org/10.1038/nature06281.

Lebow, M.A., Chen, A., 2016. Overshadowed by the amygdala: the bed nucleus of the stria terminalis emerges as key to psychiatric disorders. Mol. Psychiatry. https://doi.org/10.1038/mp.2016.1.

Levy, I., Schiller, D., 2021. Neural computations of threat. Trends Cogn Sci 25, 151–171. https://doi.org/10.1016/j.tics.2020.11.007.

Lima, S.L., Bednekoff, P.A., 1999. Temporal variation in danger drives antipredator behavior: the predation risk allocation hypothesis. Am Nat 153, 649–659. https://doi.org/10.1086/303202.

Luchsinger, J.R., Fetterly, T.L., Williford, K.M., Salimando, G.J., Doyle, M.A., Maldonado, J., Simerly, R.B., Winder, D.G., Centanni, S.W., 2021. Delineation of an insula-BNST circuit engaged by struggling behavior that regulates avoidance in mice. Nat Commun 12, 3561. https://doi.org/10.1038/s41467-021-23674-z.

Marcinkiewcz, C.A., Mazzone, C.M., D'Agostino, G., Halladay, L.R., Hardaway, J.A., Diberto, J.F., Navarro, M., Burnham, N., Cristiano, C., Dorrier, C.E., Tipton, G.J., Ramakrishnan, C., Kozicz, T., Deisseroth, K., Thiele, T.E., McElligott, Z.A., Holmes, A., Heisler, L.K., Kash, T.L., 2016. Serotonin engages an anxiety and fear-promoting circuit in the extended amygdala. Nature. https://doi.org/10.1038/nature19318.

Mazzone, C.M., Pati, D., Michaelides, M., DiBerto, J., Fox, J.H., Tipton, G., Anderson, C., Duffy, K., McKlveen, J.M., Hardaway, J.A., Magness, S.T., Falls, W.A., Hammack, S. E., McElligott, Z.A., Hurd, Y.L., Kash, T.L., 2018. Acute engagement of Gq-mediated signaling in the bed nucleus of the stria terminalis induces anxiety-like behavior. Mol. Psychiatry. https://doi.org/10.1038/mp.2016.218.

Miller, S.M., Marcotulli, D., Shen, A., Zweifel, L.S., 2019. Divergent medial amygdala projections regulate approach-avoidance conflict behavior. Nat Neurosci 22, 565–575. https://doi.org/10.1038/s41593-019-0337-z.

Mobbs, D., Yu, R., Rowe, J.B., Eich, H., FeldmanHall, O., Dalgleish, T., 2010. Neural activity associated with monitoring the oscillating threat value of a tarantula. Proc Natl Acad Sci U S A 107, 20582–20586. https://doi.org/10.1073/pnas.1009076107.

Naaz, F., Knight, L.K., Depue, B.E., 2019. Explicit and ambiguous threat processing: functionally dissociable roles of the amygdala and bed nucleus of the stria terminalis. J Cogn Neurosci 31, 543–559. https://doi.org/10.1162/jocn_a_01369.

Nguyen, A.Q., Dela Cruz, J.A., Sun, Y., Holmes, T.C., Xu, X., 2016. Genetic cell targeting uncovers specific neuronal types and distinct subregions in the bed nucleus of the stria terminalis. J Comp Neurol 524, 2379–2399. https://doi.org/10.1002/cne.23954.

Paxinos, G., Franklin, K.B.J., 2001. In: The Mouse Brain in Stereotaxic Coordinates, second ed. Academic Press, San Diego, California, USA.

Pereira, A.G., Moita, M.A., 2016. Is there anybody out there? Neural circuits of threat detection in vertebrates. Curr Opin Neurobiol 41, 179–187. https://doi.org/10.1016/j.conb.2016.09.011.

Perez-Gomez, A., Bleymehl, K., Stein, B., Pyrski, M., Birnbaumer, L., Munger, S.D., Leinders-Zufall, T., Zufall, F., Chamero, P., 2015. Innate predator odor aversion driven by parallel olfactory subsystems that converge in the ventromedial hypothalamus. Curr Biol 25, 1340–1346. https://doi.org/10.1016/j.cub.2015.03.026.

Pomrenze, M.B., Tovar-Diaz, J., Blasio, A., Maiya, R., Giovanetti, S.M., Lei, K., Morikawa, H., Woodward Hopf, F., Messing, R.O., 2019. A corticotropin releasing factor network in the extended amygdala for anxiety. J. Neurosci. 39, 1030–1043. https://doi.org/10.1523/JNEUROSCI.2143-18.2018.

Radley, J.J., Gosselink, K.L., Sawchenko, P.E., 2009. A discrete GABAergic relay mediates medial prefrontal cortical inhibition of the neuroendocrine stress response. J. Neurosci. 29, 7330–7340. https://doi.org/10.1523/JNEUROSCI.5924-08.2009.

Rale, A., Shendye, N., Bodas, D.S., Subhedar, N., Ghose, A., 2017. CART neuropeptide modulates the extended amygdalar CeA-vBNST circuit to gate expression of innate fear. Psychoneuroendocrinology. https://doi.org/10.1016/j.psyneuen.2017.08.012.

Rosen, J.B., Asok, A., Chakraborty, T., 2015. The smell of fear: innate threat of 2,5-dihydro-2,4,5-trimethylthiazoline, a single molecule component of a predator odor. Front Neurosci 9, 292. https://doi.org/10.3389/fnins.2015.00292.

Sanford, C.A., Soden, M.E., Baird, M.A., Miller, S.M., Schulkin, J., Palmiter, R.D., Clark, M., Zweifel, L.S., 2017. A central amygdala CRF circuit facilitates learning about weak threats. Neuron 93, 164–178. https://doi.org/10.1016/j.neuron.2016.11.034.

Shackman, A.J., Fox, A.S., 2016. Contributions of the central extended amygdala to fear and anxiety. J. Neurosci. https://doi.org/10.1523/JNEUROSCI.0982-16.2016.

Silva, B.A., Gross, C.T., Graff, J., 2016. The neural circuits of innate fear: detection, integration, action, and memorization. Learn Mem 23, 544–555. https://doi.org/10.1101/lm.042812.116.

Somerville, L.H., Whalen, P.J., Kelley, W.M., 2010. Human bed nucleus of the stria terminalis indexes hypervigilant threat monitoring. Biol Psychiatry 68, 416–424. https://doi.org/10.1016/j.biopsych.2010.04.002.

Takahashi, L.K., Nakashima, B.R., Hong, H., Watanabe, K., 2005. The smell of danger: a behavioral and neural analysis of predator odor-induced fear. Neurosci Biobehav Rev 29, 1157–1167. https://doi.org/10.1016/j.neubiorev.2005.04.008.

Taniguchi, H., He, M., Wu, P., Kim, S., Paik, R., Sugino, K., Kvitsiani, D., Fu, Y., Lu, J., Lin, Y., Miyoshi, G., Shima, Y., Fishell, G., Nelson, S.B., Huang, Z.J., 2011. A resource of Cre driver lines for genetic targeting of GABAergic neurons in cerebral cortex. Neuron 71, 995–1013. https://doi.org/10.1016/j.neuron.2011.07.026.

Tovote, Philip, Fadok, J.P., Lüthi, A., 2015a. Neuronal circuits for fear and anxiety. Nat. Rev. Neurosci. https://doi.org/10.1038/nrn3945.

Vong, L., Ye, C., Yang, Z., Choi, B., Chua Jr., S., Lowell, B.B., 2011. Leptin action on GABAergic neurons prevents obesity and reduces inhibitory tone to POMC neurons. Neuron 71, 142–154. https://doi.org/10.1016/j.neuron.2011.05.028.

Wallace, K.J., Rosen, J.B., 2000. Predator odor as an unconditioned fear stimulus in rats: elicitation of freezing by trimethylthiazoline, a component of fox feces. Behav Neurosci 114, 912–922. https://doi.org/10.1037//0735-7044.114.5.912.

Ye, J., Veinante, P., 2019. Cell-type specific parallel circuits in the bed nucleus of the stria terminalis and the central nucleus of the amygdala of the mouse. Brain Struct Funct 224, 1067–1095. https://doi.org/10.1007/s00429-018-01825-1.

Yehuda, R., Antelman, S.M., 1993. Criteria for rationally evaluating animal models of posttraumatic stress disorder. Biol Psychiatry 33, 479–486. https://doi.org/10.1016/0006-3223(93)90001-t.

Yu, Garcia da Silva, P., Albeanu, D.F., Li, B., 2016. Central amygdala somatostatin neurons gate passive and active defensive behaviors. J Neurosci 36, 6488–6496. https://doi.org/10.1523/JNEUROSCI.4419-15.2016.

Yu, K., da Silva, P.G., Albeanu, D.F., Li, B., 2016a. Central amygdala somatostatin neurons gate passive and active defensive behaviors. J. Neurosci. 36, 6488–6496. https://doi.org/10.1523/JNEUROSCI.4419-15.2016.

Zhong, S., Zhang, S., Fan, X., Wu, Q., Yan, L., Dong, J., Zhang, H., Li, L., Sun, L., Pan, N., Xu, X., Tang, F., Zhang, J., Qiao, J., Wang, X., 2018. A single-cell RNA-seq survey of the developmental landscape of the human prefrontal cortex. Nature. https://doi.org/10.1038/nature25980.